

Article

# Characterization of Wear and Physical Properties of Pawpaw–Glass Fiber Hybrid Reinforced Epoxy Composites for Structural Application

Isiaka Oluwole Oladele <sup>1,\*</sup>, Oluwaseun Temilola Ayanleye <sup>1</sup>, Adeolu Adesoji Adediran <sup>2,3,\*</sup>, Baraka Abiodun Makinde-Isola <sup>1</sup>, Anuoluwapo Samuel Taiwo <sup>1</sup> and Esther Titilayo Akinlabi <sup>3</sup>

<sup>1</sup> Department of Metallurgical and Materials Engineering, Federal University of Technology, Akure PMB 704, Nigeria; oluwaseunayanleye@gmail.com (O.T.A.); barakaisola@gmail.com (B.A.M.-I.); sataiwo@futa.edu.ng (A.S.T.)

<sup>2</sup> Department of Mechanical Engineering, Landmark University, Omu-Aran PMB 1001, Nigeria

<sup>3</sup> Department of Mechanical Engineering Science, University of Johannesburg, Auckland Park Campus, Johannesburg 2006, South Africa; etakinlabi@gmail.com

\* Correspondence: iooladele@futa.edu.ng (I.O.O.); adediran.adeolu@lmu.edu.ng (A.A.A.); Tel.: +234-803-467-7039 (A.A.A.)

Received: 13 February 2020; Accepted: 7 March 2020; Published: 3 July 2020



**Abstract:** In this study, wear resistance and some selected physical properties of pawpaw–glass fiber hybrid reinforced epoxy composites were investigated. Two different layers of pawpaw stem—linear and network structures—were extracted and chemically modified. Hybrid reinforced composites were developed comparatively from the two fiber structures and glass fiber using hand lay-up in an open mold production process. The wear resistance was studied via the use of a Taber Abrasion Tester while selected physical properties were also investigated. The influence of the fiber structure on the properties examined revealed that network structured pawpaw fiber was the best as reinforcement compared to the linearly structured fiber. The addition of these vegetable fibers to epoxy resin brought about improved thermal conductivity and increased the curing rate while the wear resistance of the corresponding developed composites were enhanced by 3 wt% and 15 wt% of fibers from linear and network pawpaw fibers. It was noticed that linearly structured pawpaw fiber had its best result at 3 wt% while network structured pawpaw fiber had its best result at 15 wt%.

**Keywords:** hybrid; biodegradable; polymer composite; agro-waste; environment

## 1. Introduction

The use of natural or synthetic fibers for the development of composite materials has shown significant uses in a variety of fields. In construction industries, fiber reinforced plastic (FRP) composites have been confirmed as a sustainable structural material in bridge construction. Bridge structures use FRP or FRP–concrete hybrids as primary construction materials for bridge components, such as girders, bridge decks, and slab-on-girder bridge structures. When likened to reinforced concrete (RC) decks, FRP–concrete hybrid decks revealed higher resilience with less toughness weakening under design truckloads [1]. For machine-driven applications, like mechanical gear pair, an enhancement of about 50% in the load-carrying capacity was achieved when 28% glass fiber reinforcement was added to polyoxymethylene (POM) with a lower specific wear rate when equaled to unreinforced POM [2]. Automobile body parts, such as engine hood, dashboards, and storage tanks, were mass-produced by using reinforcements from natural fibers like bagasse, flax, banana, hemp, jute, sisal, and ramie. Aerospace application involves aircraft wing boxes produced by ramie fiber composites with a reduction in weight [3]. Hybrid kenaf/glass fiber reinforced polymer composites displayed improved

mechanical properties with a resistance to rain erosion, which made the material suitable for aircraft application [4]. Carbon fiber reinforced silicon carbide is used for aircraft brakes to bear temperatures of up to 1200 °C [5]. In biomedical applications, such as dentistry and orthopedics, a variety of aramid fibers demonstrate their biomedical uses in protein immobilization that is essential for medical implants and devices. In modern orthopedic medicine, aramid fibers act as antimicrobial materials. In the marine industry, carbon fiber reinforced plastics (CFRP) display enhanced mechanical properties, like a high strength-to-weight ratio, good resistance to corrosion, fatigue, and temperature changes with a low maintenance cost making the material appropriate for marine propellers [6]. Carbon fiber skins with polymeric central sandwich composite sheets have been used for the manufacturing of entire hulls and marine craft structures [7]. Due to increased environmental consciousness and regulations, the growing request for the use nonconventional materials has leads to the development of biodegradable, sustainable, and ecofriendly materials [8–10].

In the early stage, the reinforcements being used for the development of composite materials are man-made and are also referred to as artificial fibers. They are mainly produced from silicon dioxide through a series of physical and chemical processing methods, which are too expensive for mass production. Moreover, they possess oxides of magnesium, sodium, aluminum, calcium, potassium, and boron in small quantities [11]. Among the artificial reinforcements, carbon, glass, kevlar, or aramid are commonly used by the industries due to their competitive properties. Many studies have been carried out to characterize glass and kevlar fiber reinforced composites [12–15]. Each fiber was found to be best in a specific property and glass was found to be superior for its tensile and flexural strengths, Young's modulus, density, breaking strain, cost, and accessibility. Based on these, glass fiber was used by many researchers as reinforcement in various polymeric matrix composites [16].

This research entails the development of hybrid composites with the combination of natural and artificial fibers. Composite structures consisting of more than one type of reinforcement are considered hybrid composites. Various methods of mixing these reinforcements have been reported, which comprises of stacking layers, mixing to create an interplaying hybrid, intermingling, selective placement and placing each reinforcements according to specific orientations [17].

Despite the large number of available literature on natural fibers, less attention has been given to pawpaw stem fiber in developing polymer composites. Moreover, the stem was discovered to exist in three layers, which are outer, middle, and innermost, with the outer and middle being network structured, while the innermost layer was linearly structured. In this research, the middle and innermost layers were used for the development of the hybrid composites. The fiber was extracted using a dew retting process followed by manual sorting of the different layers.

## 2. Materials and Methods

The pawpaw fiber was extracted from a pawpaw stem that was sourced from a farmland in Akure Ondo State, while short glass fiber, epoxy resin, and hardener were procured from Chemical and Allied Company in Lagos State. The short glass fiber has a length of 0.5–2.8 mm and a linear density of 2.5 g/cm<sup>3</sup>. The stem from the pawpaw tree was allowed to undergo a dew retting process for 1 month during which the action of micro-organisms and moisture on the stem aided the dissolution of the cellular tissues and pectin surrounding bast fiber bundles, thus aiding the separation of the fiber from the stem. The stem contains three layers, which include the outer layer, the middle layer (with a network structure), and the innermost layer (with a linear structure). Two of the 3 layers, as shown in Figure 1, were used in this research (network and linear structures). All the strands obtained were chemically treated with sodium hydroxide (0.5 M NaOH) using the shaking water bath operated at 50 °C for 1 h. This was done in order to increase the adhesive nature of the fiber by promoting surface roughness as well as reducing the tendency for micro-organism infection so as to preserve the fiber when incorporated into the matrix.

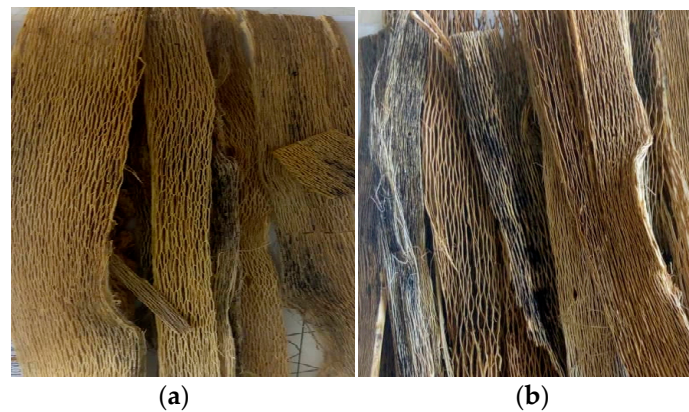


**Figure 1.** Photographic representations of chemically treated pawpaw stem fibers. (a) Extracted and treated linear fiber (b) Extracted and treated network fiber.

The composites were formed through open mold casting hand lay-up technique. The molds were properly cleansed and dried to avoid inclusions in the product and surface defects. The homogenous mixture of the epoxy resin, short glass fiber, and the hardener was accomplished through manual mixing with a wooden rod stirrer in a plastic container, which was then introduced into the mold containing the pawpaw fiber. The unreinforced epoxy matrix was also produced and used as the control sample in the research. The samples were allowed to cure at an ambient temperature of  $24 \pm 2$  °C.

A wear test was performed on the Taber Abrasion testing machine (Taber Abrasives, Model ISE AO16, TABER Industries, 455 Bryant Street, North Tonawanda, New York, NY, USA). This test was done to determine the vulnerability of the material to abrasion. The initial weights of the samples were measured and recorded as  $W_1$  after which the samples were fixed on the machine one after the other for the test. The revolution per minute of the machine was 200 rpm. At the end of each abrasion process, the final weights of the samples were measured on the electronic weighing machine and recorded. Three samples were tested for each composition and their mean values were used to ensure the accuracy and reliability according to [17]. The experiment was carried out at an ambient temperature of  $24 \pm 2$  °C and the wear resistance was calculated using Equation (1):

$$\text{Wear index} = \frac{W_1 - W_0}{\text{RPM}} \times 1000 \quad (1)$$

where  $W_1$  is the initial weight,  $W_0$  is the final weight after surface abrasion, and rpm is revolutions per minutes.

Holmarc's Lee's Disc Apparatus (Model: HO-ED-M-03) designed for the measurement of thermal conductivity in poor conductors was used in this research. The apparatus, comprising a temperature controller, contactor, thermocouple sensor, and heater, was used for the determination of the thermal behavior of the composites and the control sample. Temperature controller 1 was activated to a preset temperature value ( $T_1$ ) for disk A. The heat from the heater was transferred from disk A through the sample to disk B. The two sensors  $Th_1$  and  $Th_2$  connected to the disks were used to sense temperature changes in the metal disks. The process was set up by placing the sample in between disk A and disk B. The switch was on and disk A was preset to known temperatures that act as reference temperatures. Temperature change in disk B was noted and recorded at a regular interval until there no temperature change took place. The apparatus was switched off after taking the final readings, which were used to determine the thermal conductivity from Equations (2) and (3).

Thermal conductivity

$$K = mc_p(\theta_1 - \theta_2) \frac{4x}{\pi D^2} (T_1 - T_2) t (W/mK) \quad (2)$$

where  $m$ —mass of the disk, 0.0078 Kg;  $c_p$ —specific heat capacity of the disk, 0.91 kJ/KgK;  $\theta_1, \theta_2$ —initial and final temperature of disk B;  $D$ —diameter of the sample, 0.04 m;  $x$ —thickness of the sample, 0.003 m;  $T_1, T_2$ —temperature of disk A and B in Kelvin; and  $t$ —final time taken to reach a steady temperature.

Thermal conductance was calculated from the thermal conductivity and thickness of the material using Equation (3).

Thermal Conductance

$$C = \frac{k}{x} \text{ (W/K)} \quad (3)$$

where,  $k$ —thermal conductivity and  $x$ —thickness of the sample.

The moisture absorption in water was carried out in accordance with ASTM D5229M-12. The weights of the dry samples were reported as the initial weight of the composites. The samples were then placed in distilled water that was maintained at ambient temperatures. The samples were removed from the water, cleaned by using a dry cloth, and weighed at time intervals of 24 h for 168 h. At this time, water saturation in all the samples were noticed according to [18]. Water absorbed by the samples in (%) was calculated using Equation (4):

$$W \text{ (%) } = \frac{W_t - W_0}{W_0} \times 100 \quad (4)$$

where  $W$ —percentage of water absorption,  $W_0$  and  $W_t$ —initial weight and weight after immersion at time  $t$ , respectively.

Moisture absorption in a soil test was carried out on the specimens by oven drying at a temperature of 105 °C for 3 h, followed by weighing of the dry samples, which were then recorded as the initial weight. The samples were then buried in the soil and exhumed from the soil after 3 months, cleaned by using a dry cloth, weighed, and recorded as final weight [19]. The amount of weight loss by the samples in (%) was calculated using Equation (5).

$$W \text{ (%) } = \frac{W_t - W_0}{W_0} \times 100 \quad (5)$$

where,  $W$ —percentage weight loss,  $W_0$ —the oven dry weight, and  $W_t$ —the weight after exhumation.

The SEM images of the pawpaw fiber were taken using EVO MA 15, Carl Zeiss SMT. The samples were gold sputtered to improve electrical conductivity, while optical microscopy (Leica Galen III, S/No. 1147XP, SPATIAL TECHNOLOGIES, 5716 Burbank Cres SE, Calgary, Alberta, Canada) was used to view the fiber structure.

### 3. Results and Discussion

Figure 2a,b, Figure 3a,b, Figure 4a,b and Figure 5a,b shows optical and scanning electron microscopic images for the treated and untreated network and linearly structured pawpaw fibers. The images were examined to reveal the influence of a chemical treatment on the surface morphology of the fibers. Figures 2 and 3 reveal the images of untreated network and linear structures, respectively. Figures 2a and 3a present the optical images of the structures, which reveal the fibers as they are and can be seen without any visual aid. However, Figures 2b and 3b reveal the SEM images from where the surfaces are seen to possess some spots which were cleansed after treatment as revealed by the images in Figures 4b and 5b. It was noticed from the images that the chemical treatment was able to remove some of the fiber constituents on the surface of the fiber [20].

#### 3.1. Wear Behavior

Figure 6 shows the abrasion test results for the control (unreinforced epoxy) and the composites, respectively. Findings from these results revealed that both fiber structure and content were responsible for the enhancement of the wear resistance of the composites. Although all the composites showed improved resistance to wear, the linear pawpaw fiber (LPF)/glass fiber (GF) hybrid composites results

revealed that as the fiber content increases the wear resistance decreases. While for network pawpaw fiber (NPF)/glass fiber (GF) hybrid composites, wear resistance also decreases as the fiber content increases from 3 wt% to 9 wt%, but was followed by a decrease from 12 wt% to 15 wt% reinforcement. The wear resistance was high for network pawpaw fiber within 3–9 wt% compared to linearly structured fiber, but changed from 12 wt% to 15 wt%. Maximum enhancement was observed at 3 wt% and 15 wt% hybrid reinforced linear and network composites, respectively, with the least mass loss of about 1.3 g each. The mass loss of the control sample was the highest with a value of about 4 g. The significant reduction in the wear rate of these composites can be attributed to good bonding between the reinforcements and the epoxy matrix as well as the stiff nature of the fiber. The SEM images in Figures 4b and 5b revealed a well compacted fiber surface that can also contribute to high wear resistance observed in the developed composites. This result was in agreement with findings from previous researchers who reported that the addition of glass fiber is recommended for natural fiber based polymer composites in order to enhance the wear characteristics of the composites [21,22]. However, it was discovered from this research that the linearly structured pawpaw fiber based composite gave better wear resistance than network structure based fiber. This inference was based on the fiber volume that needed to obtain enhanced wear resistance in the developed composites in which LPF was within 3–9 wt% while NPF was within 12–15 wt%. This result revealed that less LPF volume is needed to achieve high wear resistance compared to NPF. Figures 4a and 5a show the morphologies of these fibers as revealed by optical microscopy.

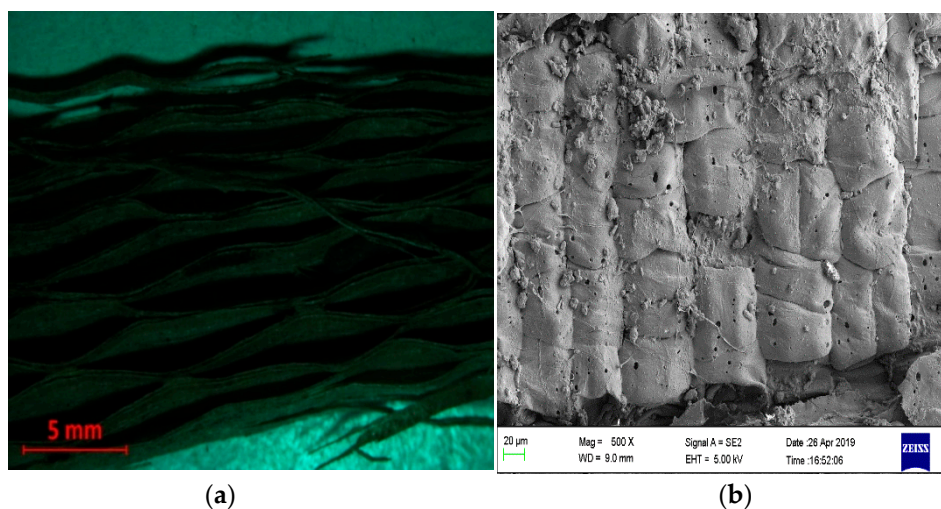


Figure 2. (a,b) Optical and SEM representation of untreated network structure pawpaw fiber.

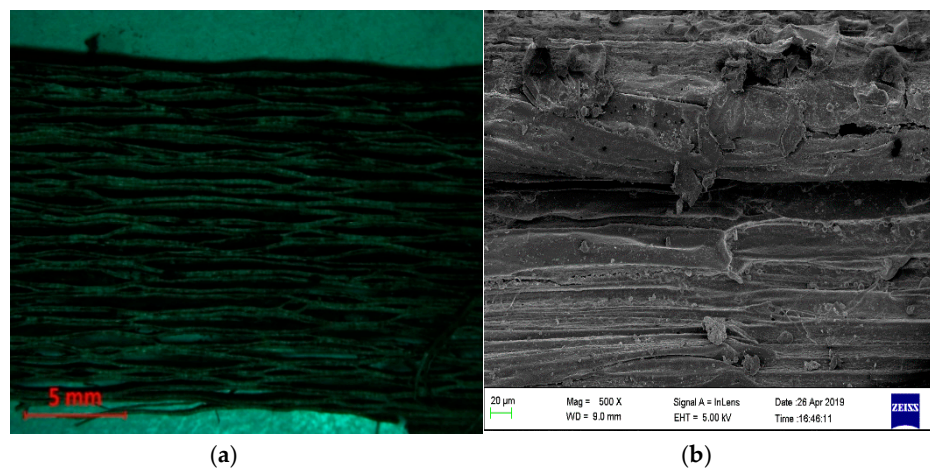


Figure 3. (a,b) Optical and SEM representation of untreated linearly structured pawpaw fiber.

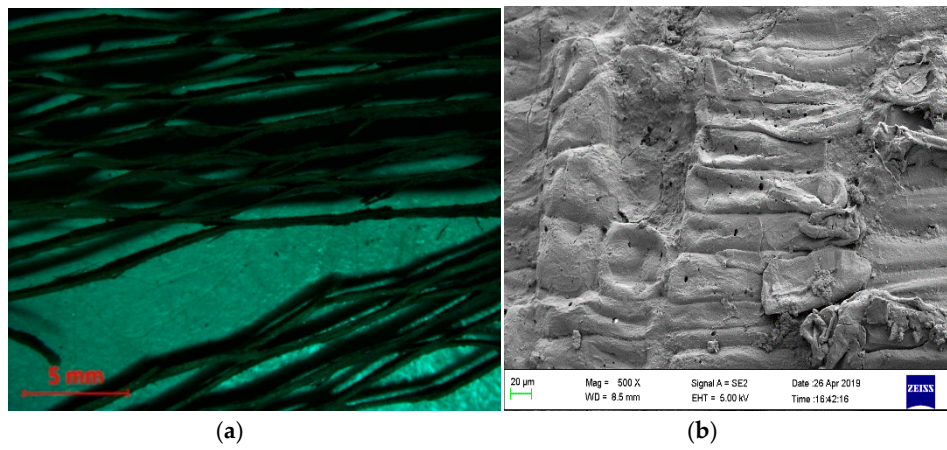


Figure 4. (a,b) Optical and SEM representation of treated network structure pawpaw fiber.

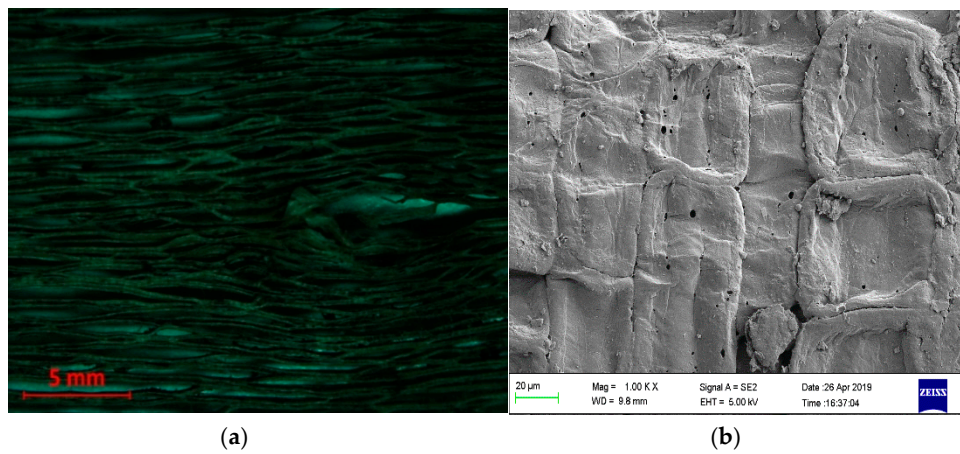


Figure 5. (a,b) Optical and SEM representation of treated linearly structured pawpaw fiber.

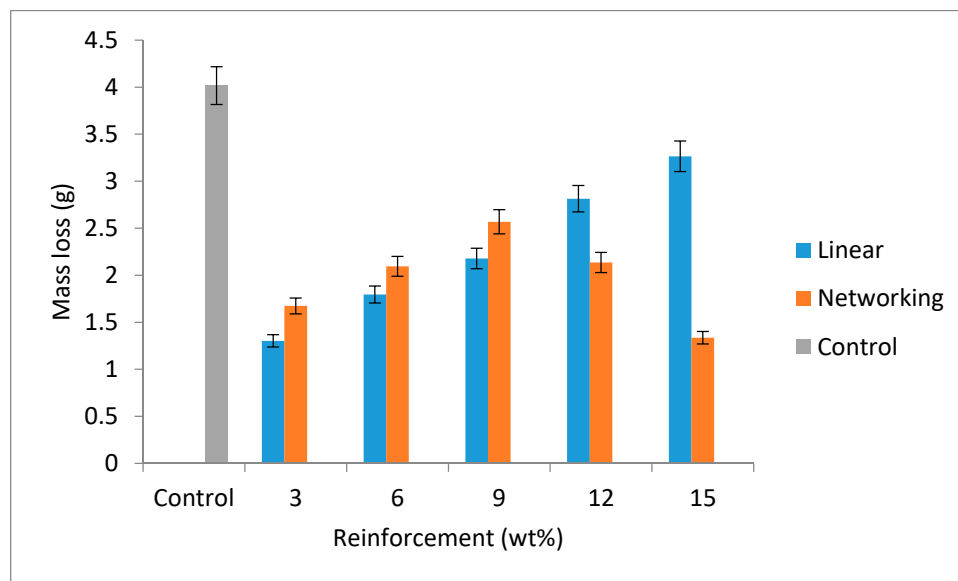
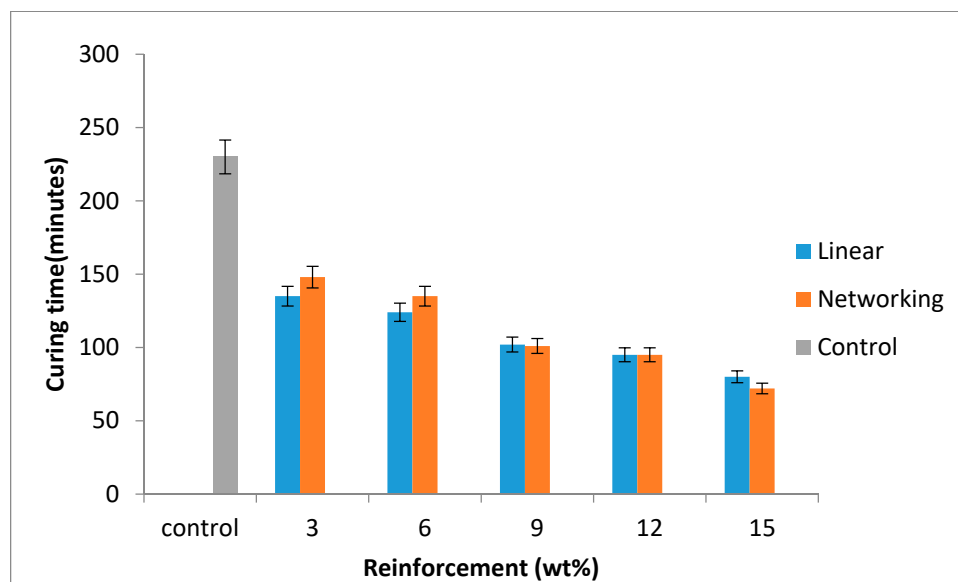


Figure 6. Variation of mass loss with wt% of reinforcement for the composites and the control sample.

### 3.2. Curing Time

Figure 7 shows the curing time chart against the weight percentage composition of both linear and networking layers as well as the control, sample which was observed at ambient temperatures. Curing time is a parameter that determines how fast the product can be developed and this has a strong influence on the production rate. It was observed that the control sample takes a longer curing time of 230 min to solidify compared to the hybrid reinforced composites. The results revealed that as the glass fiber content increases, the curing time gradually reduces for the reinforced composites. This suggests good bonding between the constituents, hence, the possibility of a high production rate. From the results, 15 wt% (glass fiber and networking pawpaw fiber) + 85 wt% (epoxy and hardener) that cured within 72 min possessed the lowest curing time. This was closely followed by hybrid composite from the same composition with linear pawpaw fiber that cured within 80 min. These results show that the higher the percentage composition of the reinforcement, the lower the curing time. According to [23], it was discovered that an increase in curing temperature to 100 °C increased mechanical properties before experiencing a drastic decrease with further increase in temperature of up to 130 °C. It was concluded that the best strength of jute/epoxy based composites was achieved at a curing temperature of 100 °C. Increase in mechanical properties due to an increase in curing temperature was also supported by various studies [24,25].



**Figure 7.** Variation of curing time (minutes) with wt% of reinforcement for the composites and the control sample.

### 3.3. Thermal Conductivity

Thermal conductivity of polymer based materials is of great interest to electronic industries. Polymers are poor heat conductors due to the absence of free electrons for conduction mechanisms. The thermal insulating potential of polymers is rated by measuring the thermal conductivity. Polymers in general have low thermal conductivity since they have an isolated structure of individual chains. Discontinuities lead to phonon scattering that when even the backbone is thermally conductive, it is rather difficult to make the entire polymer a good thermal conductor. Epoxy was the major polymer being used for electronic applications and there is a need to improve on the electrical properties of the material. Thermal conductivity of developed composites and control sample results were shown in Figure 8. Low thermal conductivity of polymers is one of the major setbacks for its application in flexible electronics due to inadequate heat spreading capability. Therefore, developing biodegradable epoxy based composite for such an application is a good approach. The thermal conductivity of

polymer is greatly influenced by its morphology; therefore, thermal conductivity of polymer based materials can be enriched by improving the alignment of polymer chains [26–28]. An investigation carried out on the relationship between the thermal conductivity of composite reinforced with LPF/GF and NPF/GF morphology, showed that the thermal conductivity of the samples increases as the weight percentage of reinforcement increases for all samples. However, thermal conductivity was highly enhanced by network pawpaw fiber than linear pawpaw fiber, which also corroborates the submission that morphology has great influence on thermal conductivity of polymer materials. As it can be seen from the results, the thermal conductivity of the composite samples with network PF/GF was enhanced more than linear PF/GF due to the differences in their morphologies. While the thermal conductivity of epoxy was 0.62 W/mK, the thermal conductivity of the best sample from the network pawpaw fiber/glass fiber hybrid composite from 15 wt% reinforcement was 1.41 W/mk. The observed enhanced conductivity in network structure based composites (Figure 8) was due to the network nature of the fiber as shown in Figure 4a. The interconnectivity that exists in the network structure might likely encourage easy heat flow within the materials compared to the linear structure in Figure 5a. These values were in close range with the thermal conductivities of concrete mixed with recycled HDPE, LDPE, PP, and PET, which have thermal conductivities of about 0.74–0.96, 0.72–0.86, 0.84–0.94 and 0.95–1.02 W/(mK), respectively [29].

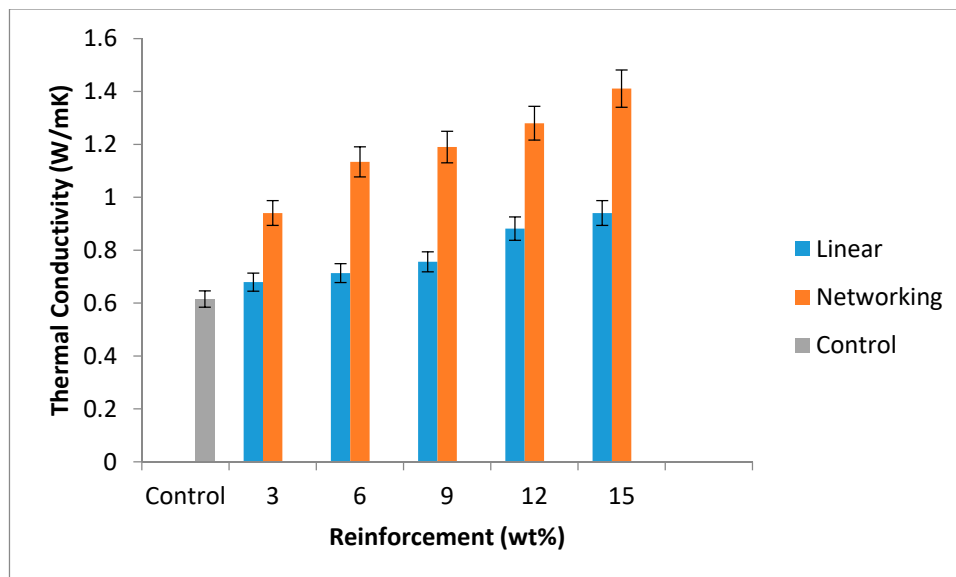


**Figure 8.** Variation of the thermal conductivity result against percentage composition samples of both the linear and networking layer as well as the control sample.

### 3.4. Moisture Absorption in Soil and Water Comparison

The effect of moisture absorption on the materials is essential in order to know how the developed composites will respond when they come in contact with water directly or in a soil environment. Figure 9 shows the various responses from these environments. The moisture absorption in soil was high compared to that of water. This may be due to many factors, such as the residence time, temperature variation, and the presence of micro-organisms in the soil. More absorption indicates a higher potential for degradation. Therefore, degradation is highly promoted in the soil environment than in the water environment due to the harsh environmental conditions of the soil. This revealed that polymer composites for underground applications should be highly protected against degradation due to the prevailing activities that such materials may likely encounter in service. The effects of the fiber structure and weight fractions were not well pronounced in the soil environment since the differences in the values were marginal in all weight fractions. However, in the water environment, the reverse was the case: linear pawpaw fiber/glass fiber hybrid reinforced composites absorbed more

water than network pawpaw fiber/glass fiber hybrid reinforced composites. Furthermore, there is a substantial increase in the moisture content with increase in weight fraction and immersion time. The moisture content of the control sample in both media was low compared to the developed composites. The moisture absorption of the control was 0.26% after 144 h in water and 1.29% after three months in soil. This observation was due to the hydrophobic nature of the polymer as stated by previous researchers [30,31]. This, however, showed that biodegradable materials need to be added to polymers in order for them to be able to degrade after use. Nowadays, the attention of researchers worldwide is on how to ensure a proper disposal of used polymer products [32–34]. Therefore, there is a need to synergize between the required properties and the disposal mode for the sake of the environment.

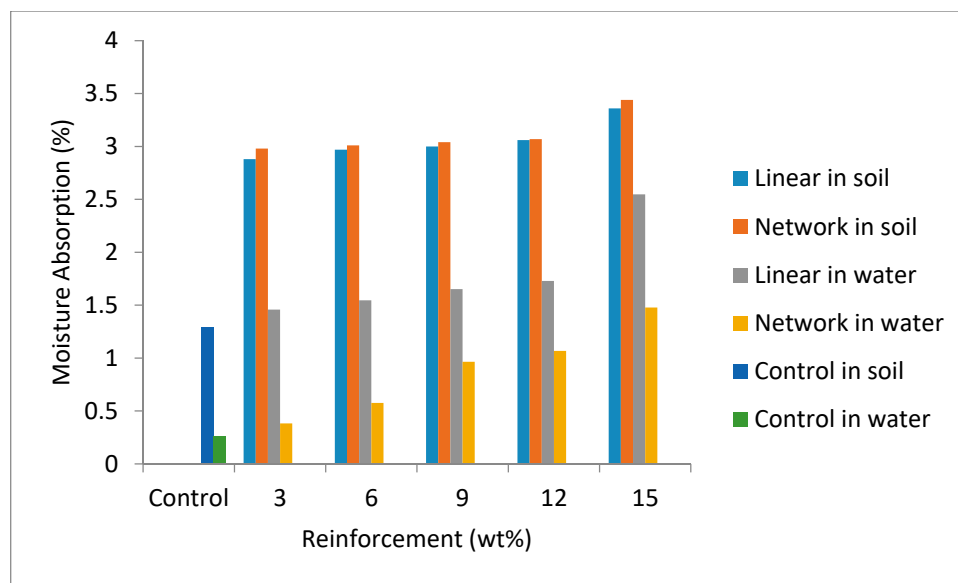


**Figure 9.** Variation of moisture content in water and soil for the developed composites and the control sample.

Considering results from this research (Figures 6–8), it was noticed that it is advantageous to add biodegradable materials to polymer as reinforcement in order to improve the properties and, hence, the potential for composite degradation after use [35]. For the moisture absorption results with respect to the composites, 3 wt% network pawpaw fiber/glass fiber hybrid composite has a low value of 0.38%, while for soil, 3 wt% linear pawpaw fiber/glass fiber hybrid composite had the best result with a value of 2.88%. There is a general substantial increase in absorption in both media, which is due to the hydrophilic nature of natural fiber material.

#### 4. Conclusions

The findings from the research have revealed that improved surface morphology was achieved from the chemical treatment carried out to modify the surface of the pawpaw fiber as well as promote good fiber/matrix interfacial adhesion.

The influence of the fiber structure on the examined properties revealed that network structured pawpaw fiber was the best for reinforcement compared to the linearly structured fiber, though, they both gave promising results. Wear resistance of the developed composites were enhanced by 3 wt% and 15 wt% fibers from linear and network pawpaw fibers, respectively. Curing time and thermal conductivity were best from the 15 wt% network pawpaw fiber, while moisture absorption was best with 3 wt% from both network and linear pawpaw fibers with respect to the composites in both soil and water environments. It was noticed that linearly structured pawpaw fiber gave the best result at 3 wt%, while network structured pawpaw fiber gave the best result at 15 wt%. It was revealed

that this agro-waste can be used to improve the curing rate during production as well as promote the development of epoxy composite materials with enhanced wear resistance and thermal conductivity.

**Author Contributions:** Conceptualization, I.O.O.; methodology, I.O.O.; software, O.T.A. and B.A.M.-I.; validation, I.O.O., O.T.A., A.A.A., B.A.M.-I., A.S.T. and E.T.A.; formal analysis, O.T.A., A.A.A., B.A.M.-I., A.S.T. and E.T.A.; investigation, I.O.O., O.T.A., A.A.A., B.A.M.-I., A.S.T. and E.T.A.; resources, I.O.O., E.T.A. and A.A.A.; data curation, B.A.M.-I. and O.T.A.; writing—original draft, I.O.O., O.T.A., A.A.A., B.A.M.-I., A.S.T. and E.T.A.; draft preparation, I.O.O., O.T.A., A.A.A., B.A.M.-I., A.S.T. and E.T.A.; writing—review & editing, I.O.O., O.T.A., A.A.A., B.A.M.-I., A.S.T. and E.T.A.; visualization, I.O.O., O.T.A., A.A.A., B.A.M.-I., A.S.T. and E.T.A.; supervision, I.O.O. and E.T.A.; project administration, I.O.O. and E.T.A.; funding acquisition, I.O.O. and A.A.A. All authors have read and agreed to the published version of the manuscript.

**Funding:** The APC was funded by Landmark University, Omu-Aran, Kwara State, Nigeria.

**Acknowledgments:** The authors appreciate the support from the Landmark University Centre for Research, Innovation and Development (LUCRID) for this research.

**Conflicts of Interest:** The authors declare no conflict of interest.

## References

- Cheng, L.; Karbhari, V.M. New bridge systems using FRP composites and concrete: A state-of-the-art review. *Prog. Struct. Eng. Mater.* **2006**, *8*, 143–154. [[CrossRef](#)]
- Mao, K.; Greenwood, D.; Ramakrishnan, R.; Goodship, V.; Shrouti, C.; Chetwynd, D.; Langlois, P. The wear resistance improvement of fibre reinforced polymer composite gears. *Wear* **2019**, *426*, 1033–1039. [[CrossRef](#)]
- Boegler, O.; Kling, U.; Empl, D.; Isikveren, A. Potential of sustainable materials in wing structural design. In Proceedings of the Deutscher Luft- und Raumfahrtkongress, München, Germany, 16–18 September 2014; pp. 16–18.
- Arockiam, N.J.; Jawaid, M.; Saba, N. Sustainable bio composites for aircraft components. In *Sustainable Composites for Aerospace Applications*; Woodhead Publishing: Sawston, UK; Cambridge, UK, 2018; pp. 109–123.
- Fan, S.; Yang, C.; He, L.; Du, Y.; Krenkel, W.; Greil, P.; Travitzky, N. Progress of ceramic matrix composites brake materials for aircraft application. *Rev. Adv. Mater. Sci.* **2016**, *44*, 313–325.
- Kumar, A.; Lal, K.G.; Anantha, S.V. Design and Analysis of a Carbon Composite Propeller for Podded Propulsion. In Proceedings of the Fourth International Conference in Ocean Engineering (ICOE2018), Chennai, India, 18–21 February 2018; Lecture Notes in Civil Engineering 22. Springer: Berlin/Heidelberg, Germany, 2018.
- Verma, D.; Goh, K.L. Natural fiber-reinforced polymer composites. In *Biomass, Biopolymer-Based Materials, and Bioenergy: Construction, Biomedical, and Other Industrial Applications*; Woodhead Publishing: Sawston, UK; Cambridge, UK, 2019; pp. 51–73.
- Qamhia, I.I.; Shams, S.S.; El-Hajjar, R.F. Quasi-isotropic triaxially braided cellulose-reinforced composites. *Mech. Adv. Mater. Struct.* **2015**, *22*, 988–995. [[CrossRef](#)]
- Arrakhiz, F.; El Achaby, M.; Malha, M.; Bensalah, M.; Fassi-Fehri, O.; Bouhfid, R. Mechanical and thermal properties of natural fibers reinforced polymer composites: Doum/low density polyethylene. *Mater. Des.* **2013**, *43*, 200–205. [[CrossRef](#)]
- Thakur, V.K.; Thakur, M.K. Processing and characterization of natural cellulose fibers/thermoset polymer composites. *Carbohydr. Polym.* **2014**, *109*, 102–117. [[CrossRef](#)]
- Alireza, S.; Ghasemian, A. Water Absorption and Thickness Swelling Behavior of Polypropylene Reinforced with Hybrid Recycled Newspaper and Glass Fiber. *Appl. Compos. Mater.* **2010**, *17*, 183–193.
- Ou, Y.; Zhu, D.; Zhang, H.; Huang, L.; Yao, Y.; Li, G.; Mobasher, B. Mechanical characterization of the tensile properties of glass fiber and its reinforced polymer (GFRP) composite under varying strain rates and temperatures. *Polymers* **2016**, *8*, 196. [[CrossRef](#)]
- Asi, O. Mechanical properties of glass-fiber reinforced epoxy composites filled with Al<sub>2</sub>O<sub>3</sub> particles. *J. Reinf. Plast. Compos.* **2008**, *28*, 2861–2867. [[CrossRef](#)]
- Singla, M.; Chawla, V. Mechanical properties of epoxy resin-fly ash composite. *J. Min. Mater. Charact. Eng.* **2010**, *9*, 199–210. [[CrossRef](#)]
- Warbhe, N.O.; Shrivastava, R.; Adwani, P.S. Mechanical properties of kevlar/jute reinforced epoxy composite. *Int. J. Innov. Res. Sci. Eng. Technol.* **2016**, *5*, 16407–16418.

16. Pegoretti, A.; Fabbri, E.; Migliaresi, C.; Pilati, F. Intraply and interply hybrid composites based on E-glass and poly (vinyl alcohol) woven fabrics: Tensile and impact properties. *Polym. Int.* **2004**, *53*, 1290–1297. [[CrossRef](#)]
17. Oladele, I.O.; Agbabiaka, O.G.; Adediran, A.A.; Akinwekomi, A.D.; Balogun, A.O. Structural performance of poultry eggshell derived hydroxyapatite based high density polyethylene bio-composites. *Heliyon* **2019**, *5*, 1–7. [[CrossRef](#)]
18. Daramola, O.O.; Akinwekomi, A.D.; Adediran, A.A.; Akindote-White, O.; Sadiku, E.R. Mechanical performance and water uptake behaviour of treated bamboo fibre-reinforced high-density polyethylene composites. *Heliyon* **2019**, *5*, 1–6. [[CrossRef](#)] [[PubMed](#)]
19. Oladele, I.O.; Adediran, A.A.; Akinwekomi, A.D.; Adara, P.P. Mathematical models for evaluating the influence of degradation on the tensile and flexural properties of palm kernel shell ash/epoxy composites. *Mater. Technol.* **2019**, *53*, 763–769. [[CrossRef](#)]
20. Oladele, I.O.; Omotoyinbo, J.A.; Adewara, J.O.T. Investigating the Effect of Chemical Treatment on the Constituents and Tensile Properties of Sisal Fibre. *J. Miner. Mater. Charact. Eng.* **2010**, *9*, 569–582. [[CrossRef](#)]
21. Shalwan, A.; Yousif, B.F. Influence of date palm fibre and graphite filler on mechanical and wear characteristics of epoxy composites. *Mater. Des.* **2014**, *59*, 264–273. [[CrossRef](#)]
22. Vina, J.; Garcia, M.A.; Castrillo, M.A.; Vina, I.; Arguelles, A. Wear behavior of a Glass Fiber-Reinforced PEI Composite. *J. Thermoplast. Compos. Mater.* **2008**, *21*, 279–286. [[CrossRef](#)]
23. Jai, I.P.S.; Sehijpal, S.; Vikas, D. Effect of Curing Temperature on Mechanical Properties of Natural Fiber Reinforced Polymer Composites. *J. Nat. Fibers* **2018**, *15*, 687–696.
24. Ramesh, M.; Sri Ananda Atreya, T.; Aswin, U.S.; Eashwar, H.; Deepa, C. Processing and mechanical property evaluation of banana fiber reinforced polymer composites. *Procedia Eng.* **2014**, *97*, 563–572. [[CrossRef](#)]
25. Srinivasan, V.S.; Rajendra Boopathy, S.; Sangeetha, D.; Vijaya Ramnath, B. Evaluation of mechanical and properties of banana–flax based natural fibre composite. *Mater. Des.* **2014**, *60*, 620–627. [[CrossRef](#)]
26. Wang, Z.L. Self-powered nanosensors and nanosystems. *J. Adv. Mater.* **2012**, *24*, 280–285. [[CrossRef](#)] [[PubMed](#)]
27. Han, C.; Li, Z.; Dou, S. Recent progress in thermoelectric materials. *Chin. Sci. Bull.* **2014**, *59*, 2073–2091. [[CrossRef](#)]
28. Chen, H.; Ginzburg, V.V.; Yang, J.; Yang, Y.; Liu, W.; Huang, Y.; Du, L.; Chen, B. Thermal conductivity of polymer-based composites: Fundamentals and applications. *Prog. Polym. Sci.* **2016**, *59*, 41–85. [[CrossRef](#)]
29. Artid, P.; Manaskorn, R.; Methi, W.; Watanachai, S. Potential Use of Plastic Wastes for Low Thermal Conductivity Concrete. *Materials* **2018**, *11*, 1938.
30. Sanjeevamurthy, G.C.; Srinivas, G.R. Sisal/coconut coir natural fibers-epoxy composites: Water absorption and mechanical properties. *Int. J. Eng. Innov. Technol.* **2014**, *2*, 166–170.
31. Bhaskar, J.; Singh, V.K. Water absorption and compressive properties of coconut shell particle reinforced-epoxy composite. *J. Mater. Environ. Sci.* **2013**, *4*, 113–118.
32. Oladele, I.O.; Abegunde, O.O.; Masud, A.O. Flexural, water absorption and wear responses of green composites from bio-resources. *Afr. J. Sci. Technol. Innov. Dev.* **2018**, *10*, 1–6. [[CrossRef](#)]
33. Adediran, A.A.; Alaneme, K.K.; Oladele, I.O.; Akinlabi, E.T. Structural Characterization of Silica based Carbothermal Derivatives of Rice Husk. *Procedia Manuf.* **2019**, *35*, 436–441. [[CrossRef](#)]
34. Faola, A.E.; Oladele, I.O.; Adewuyi, B.O.; Oyetunji, A. Development of Biodegradable High Density Polyethylene Composite for Structural Application. *Ann. Fac. Eng. Hunedoara-Int. J. Eng.* **2019**, *2*, 37–44.
35. Oladele, I.O.; Akinwekomi, A.D.; Agbabiaka, O.G.; Oladejo, M.O. Influence of Biodegradation on the tensile and Wear Resistance Properties of Bio-Derived CaCO<sub>3</sub>/Epoxy Composites. *J. Polym. Res.* **2019**, *26*, 1–9. [[CrossRef](#)]

